Video Article

In vitro Mesothelial Clearance Assay that Models the Early Steps of Ovarian Cancer Metastasis

Rachel A. Davidowitz[1], Marcin P. Iwanicki[1], Joan S. Brugge[1]

[1]Department of Cell Biology, Harvard Medical School

Correspondence to: Joan S. Brugge at joan_brugge@hms.harvard.edu

Abstract

Ovarian cancer is the fifth leading cause of cancer related deaths in the United States[1]. Despite a positive initial response to therapies, 70 to 90 percent of women with ovarian cancer develop new metastases, and the recurrence is often fatal[2]. It is, therefore, necessary to understand how secondary metastases arise in order to develop better treatments for intermediate and late stage ovarian cancer. Ovarian cancer metastasis occurs when malignant cells detach from the primary tumor site and disseminate throughout the peritoneal cavity. The disseminated cells can form multicellular clusters, or spheroids, that will either remain unattached, or implant onto organs within the peritoneal cavity[3] (Figure 1, Movie 1).

All of the organs within the peritoneal cavity are lined with a single, continuous, layer of mesothelial cells[4-6] (Figure 2). However, mesothelial cells are absent from underneath peritoneal tumor masses, as revealed by electron micrograph studies of excised human tumor tissue sections[3,5-7] (Figure 2). This suggests that mesothelial cells are excluded from underneath the tumor mass by an unknown process.

Previous *in vitro* experiments demonstrated that primary ovarian cancer cells attach more efficiently to extracellular matrix than to mesothelial cells[8], and more recent studies showed that primary peritoneal mesothelial cells actually provide a barrier to ovarian cancer cell adhesion and invasion (as compared to adhesion and invasion on substrates that were not covered with mesothelial cells)[9,10]. This would suggest that mesothelial cells act as a barrier against ovarian cancer metastasis. The cellular and molecular mechanisms by which ovarian cancer cells breach this barrier, and exclude the mesothelium have, until recently, remained unknown.

Here we describe the methodology for an *in vitro* assay that models the interaction between ovarian cancer cell spheroids and mesothelial cells *in vivo* (Figure 3, Movie 2). Our protocol was adapted from previously described methods for analyzing ovarian tumor cell interactions with mesothelial monolayers[8-16], and was first described in a report showing that ovarian tumor cells utilize an integrin –dependent activation of myosin and traction force to promote the exclusion of the mesothelial cells from under a tumor spheroid[17]. This model takes advantage of time-lapse fluorescence microscopy to monitor the two cell populations in real time, providing spatial and temporal information on the interaction. The ovarian cancer cells express red fluorescent protein (RFP) while the mesothelial cells express green fluorescent protein (GFP). RFP-expressing ovarian cancer cell spheroids attach to the GFP-expressing mesothelial monolayer. The spheroids spread, invade, and force the mesothelial cells aside creating a hole in the monolayer. This hole is visualized as the negative space (black) in the GFP image. The area of the hole can then be measured to quantitatively analyze differences in clearance activity between control and experimental populations of ovarian cancer and/ or mesothelial cells. This assay requires only a small number of ovarian cancer cells (100 cells per spheroid X 20-30 spheroids per condition), so it is feasible to perform this assay using precious primary tumor cell samples. Furthermore, this assay can be easily adapted for high throughput screening.

Video Link

The video component of this article can be found at http://www.jove.com/video/3888/

Protocol

1. Ovarian Cancer Cell Spheroid Formation

1. RFP-expressing ovarian cancer cells are cultured in 10% Base Medium (a custom cell culture medium containing a 50:50 mixture of 199 and MCDB105, 10% inactivated fetal bovine serum and 1% pen-strep). To express RFP in unlabeled ovarian cancer cells, transfect the cells with a plasmid containing RFP and select for cells expressing RFP. Alternatively, viral vectors can be used to transiently express fluorescent proteins, or cells can be pre-incubate with a red fluorescent cell tracker dye (Invitrogen).
2. Prior to forming of ovarian cancer spheroids, it is necessary to prepare low-adhesion 96 well round bottom culture dishes. To produce the low-adhesion culture plates, 30μl poly-HEMA (6mg polyhydroxyethylmethacrylate in 1 ml 95% EtOH) solution is added to each well of a 96 well Corning cell culture dish. The 96 well plates are incubated in a 37°C non-humidified incubator to evaporate the ethanol, leaving a film of poly-

HEMA on each well. This poly-HEMA film prevents cells from attaching to the bottom of the well, forcing the cells to grow in suspension[18]. [Alternatively, Ultra-Low Attachment culture plates (Corning) can be used instead of poly-HEMA coated dishes.]

3. After the low-adhesion culture plates are prepared, trypsinize a plate of ovarian cancer cells, pellet the cells in a tabletop centrifuge (Heraeus) at 900 RCF for 3 minutes, aspirate the supernatant and re-suspend in 10% Base Medium.
4. Count the cells using a hemocytometer.
5. Adjust the concentration of cells such that there are 100 cells per 50μl of 10% Base Medium.
6. Add 50μl of the uniformly suspended diluted cell suspension to each well of the 96 well poly-HEMA coated culture dish.
7. Incubate the 96 well plate in a 37°C cell culture incubator for 16 hours (this amount of time should be increased or decreased depending on the amount of time it takes for a particular cell line to form multicellular spheroids or desired experimental conditions) to allow the ovarian cancer cells to cluster together, forming a single multicellular spheroid in each well. Some tumor cells can undergo apoptosis during this period, so it is important to choose a time prior to induction of apoptosis.

2. Mesothelial Cell Monolayer Formation

1. In a cell culture hood, pre-coat the wells of a 6 well glass-bottom MatTek dish with fibronectin by adding 2mL of a 5μg fibronectin/ mL PBS solution to each well of the dish and incubating at room temperature for 30 minutes. The optical quality of the glass-bottoms in MatTek dishes allow for high-resolution microscopic imaging.
2. GFP-expressing mesothelial cells are cultured in 10% Base Medium. Trypsinize a plate of mesothelial cells, spin down in a tabletop centrifuge (Heraeus) at 900RPM for 3 minutes, aspirate the supernatant, and re-suspend in 10% Base Medium. The mesothelial cells used here were already expressing GFP when they were obtained, but unlabeled mesothelial cells can be produced by transfecting with a plasmid containing GFP cDNA, or preincubating the cells in a green fluorescent cell tracker dye (Invitrogen).
3. After the 30-minute fibronectin incubation (in step 2.1), wash the wells of the MatTek dish with 2mL PBS.
4. Aspirate the PBS and plate 6 x10^5 mesothelial cell per well in each well of the 6 well MatTek dish. Incubate the MatTek dish in a 37°C cell culture incubator overnight to allow the mesothelial cells to attach to the dish and form a monolayer.

3. Mesothelial Cell Clearance Assay

1. Use a pipet to collect the ovarian cancer spheroids from the 96 well poly-HEMA coated plate.
2. Aspirate the medium from one well of the 6 well MatTek dish containing a mesothelial cell monolayer. Wash once with 2mL PBS. Add all of the spheroids from the 96 well plate to one well of the MatTek dish (~3x the number of spheroids that are going to be imaged to account for spheroids landing on the part of the dish that cannot be imaged).
3. Place the MatTek dish on the stage of an inverted widefield fluorescence microscope capable of performing time-lapse imaging for the duration of at least 8 hours. Use a motorized stage to image multiple positions in the dish, with multiple spheroid intercalation events, in a single experiment. We use a Nikon Ti-E Inverted Motorized Widefield Fluorescence time-lapse microscope with integrated Perfect Focus System and low [20x-0.75 numerical aperture (NA)] magnification/NA differential interference contrast (DIC) optics, a Nikon halogen transilluminator with 0.52 NA long working distance (LWD) condenser, Nikon fast (<100-millisecond switching time) excitation and emission filters (GFP Ex 480/40, Em 525/50, RFP-mCherry Ex 575/50 Em 640/50), Sutter fast transmitted and epifluorescence light path Smart Shutters, a Nikon linear-encoded motorized stage, a Hamamatsu ORCA-AG cooled charge-coupled device (CCD) camera, a custom-built microscope incubation chamber with temperature and CO_2 control, Nikon NIS-Elements AR software version 3, and a TMC vibration isolation table.
4. The ovarian cancer cell spheroids will settle to the bottom of dish and attach to the mesothelial cell monolayer. Collect GFP, RFP and phase images of 20+ spheroid/monolayer interactions, every 10 minutes, for 8 hours.
5. The RFP-expressing ovarian cancer cell spheroids will invade into the GFP-expressing mesothelial cell monolayer creating a hole in the monolayer. After 8 hours, measure the sizes of the holes by tracing the black holes in the GFP images using Elements software (or another suitable software such as image J) . Normalize the hole size to the initial spheroid size by dividing the hole size at 8 hours by the size of the spheroid in the corresponding RFP image at time zero. In this example, the hole size was only measured once, but it can be measured multiple times throughout the eight hour experiment to better understand the dynamics of intercalation.

4. Representative Results

In this example, we compared the mesothelial clearance ability of OVCA433 ovarian cancer cell spheroids that have attenuated expression of talin-1 to control OVCA433 spheroids. OVCA433 spheroids from each group were added to a MatTek dish containing ZT mesothelial cell monolayers. Six spheroids from each group were imaged every 10 minutes for eight hours (Figure 4, Movie 3, Movie 4). The holes produced in the monolayer by the spreading spheroids were measured and six positions from each group were averaged. Figure 4 shows that the average clearance area created by talin 1 knockdown spheroids was significantly smaller than the average area created by control spheroids, suggesting that talin is required for mesothelial clearance by OVCA433 ovarian cancer spheroids.
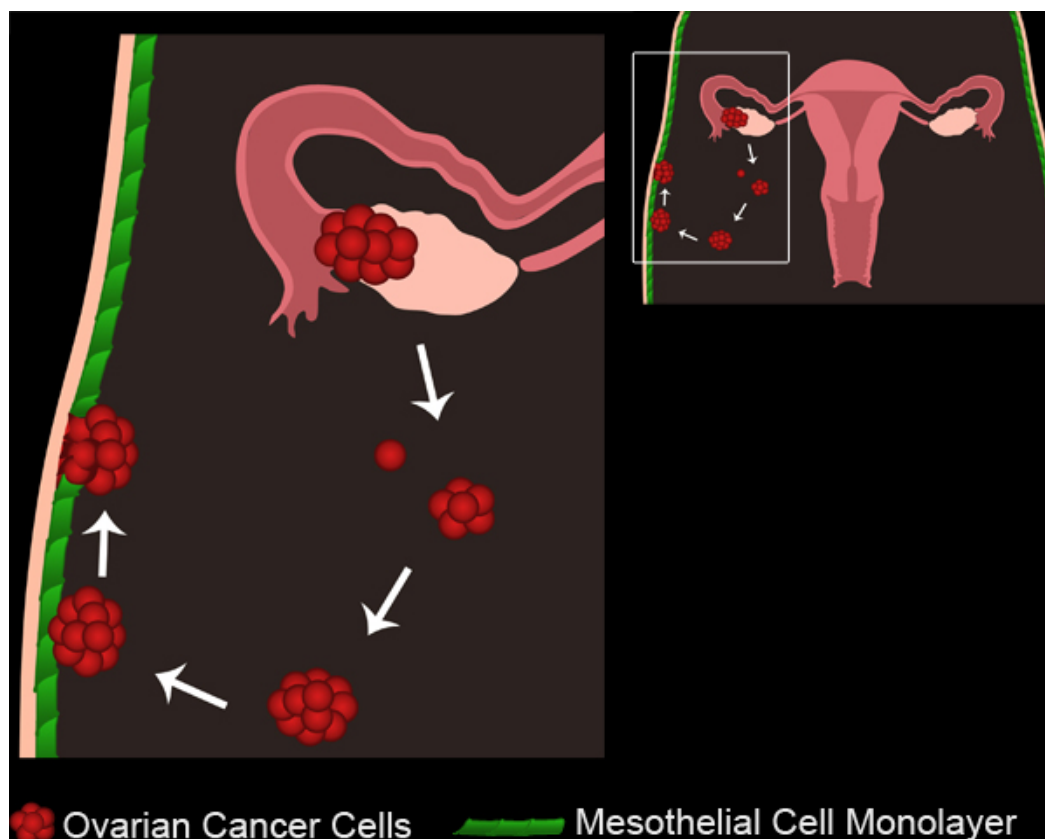
Figure 1. Ovarian Cancer Metastasis. Primary ovarian tumors develop either from the ovarian surface epithelium or fallopian tubes. Tumor cells/clusters break off from the primary tumor and collect in the peritoneal cavity. Tumor cells can then aggregate to form multicellular spheroids. Spheroids then attach to the mesothelial cell monolayers lining the peritoneal cavity. The mesothelial cells are excluded from underneath the attached ovarian cancer spheroid, allowing the spheroids to gain access to the underlying basement membrane.

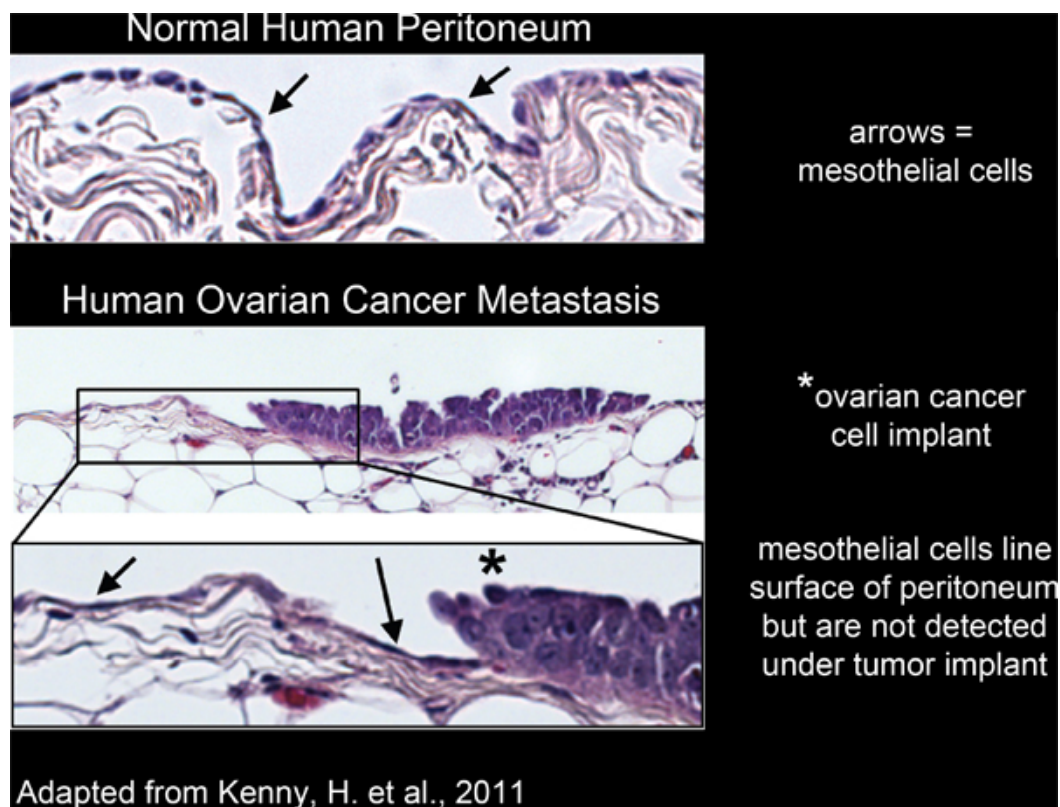**Movie 1.** Ovarian Cancer Metastasis. Click here to view movie.

Figure 2. Mesothelial cells line the surface of human peritoneal tissue and are excluded from underneath ovarian cancer cell implants.
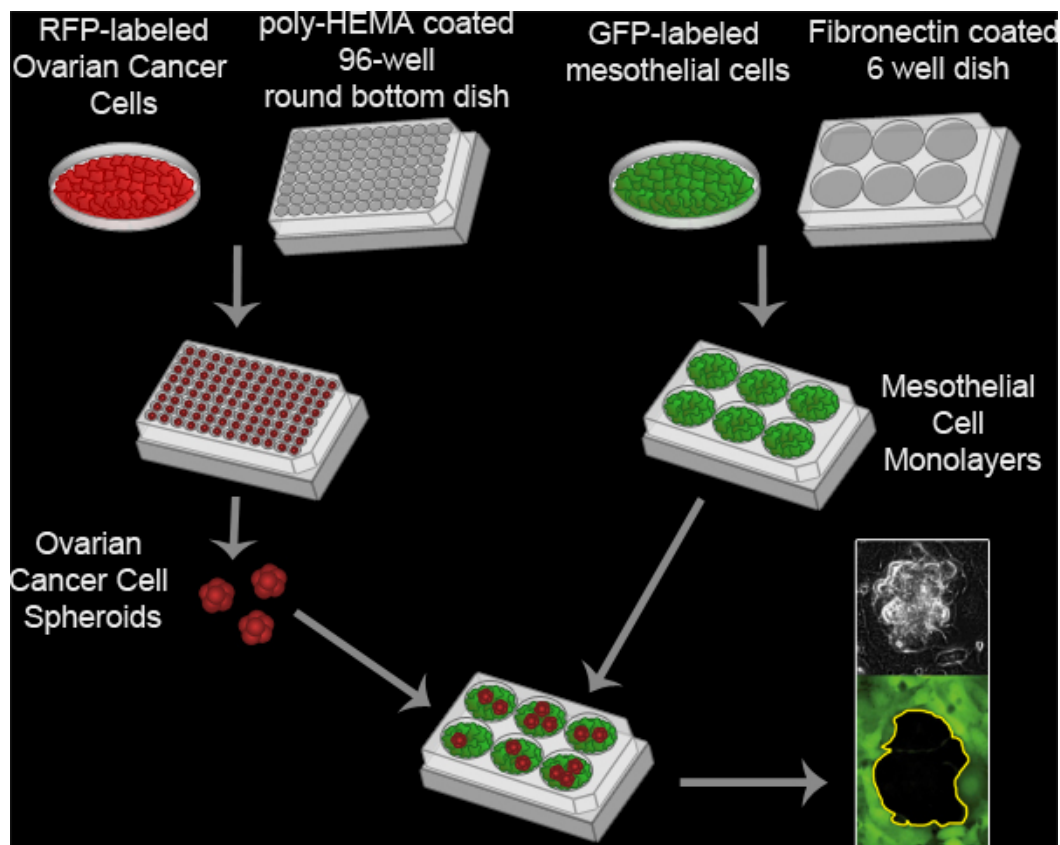
Figure 3. Mesothelial Clearance Assay. Ovarian cancer spheroids are formed by incubating 100 RFP-expressing ovarian cancer cells per well in a poly-HEMA coated 96 well round bottom culture dish at 37°C for 16 hours. Poly-HEMA prevents the cells from attaching to the culture dish, allowing the cells to remain in suspension and adhere to one another to form a single cluster per well. Mesothelial cell monolayers are prepared by plating 6×10^5 mesothelial cells per well in a fibronectin coated 6 well MatTek dish and incubating the plate at 37°C for 16 hours. The spheroids are then transferred to the MatTek dish with the mesothelial monolayer and the two cell populations are imaged every 10 minutes for 8 hours using a Nikon Ti-E Inverted Motorized Widefield Fluorescence time-lapse microscope and Elements software.

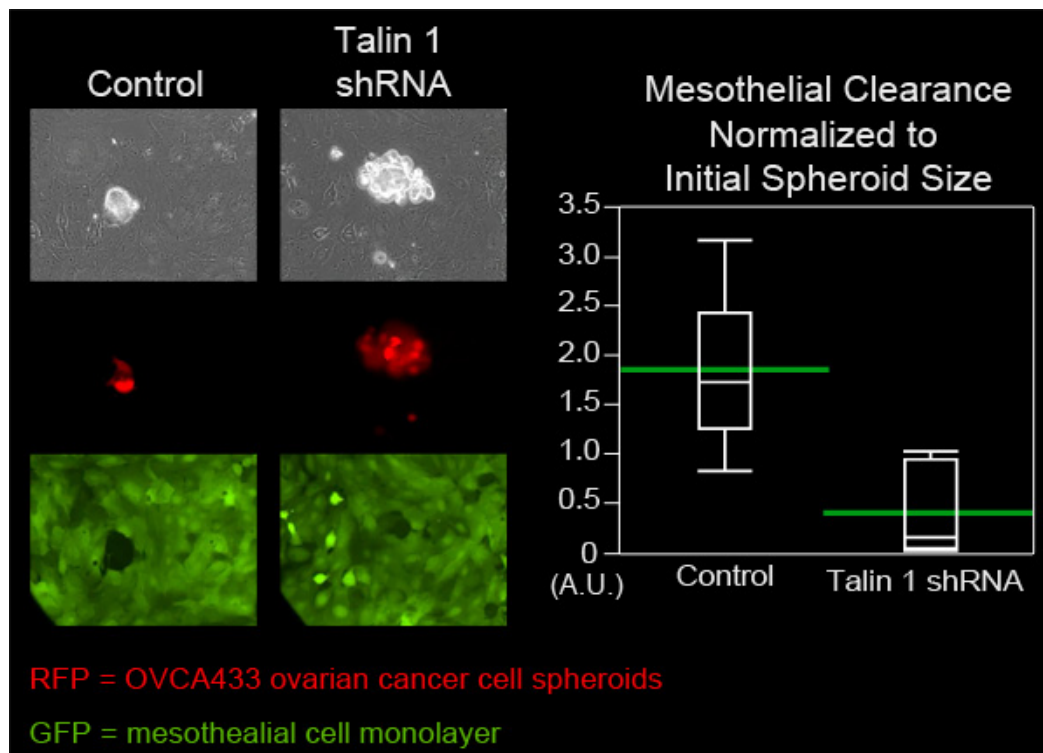**Movie 2.** Mesothelial Clearance Assay. Click here to view movie.

Figure 4. Attenuation of talin 1 expression in OVCA433 spheroids decreases mesothelial clearance ability. OVCA433 spheroids (red) with and without attenuated expression of talin 1 were allowed to attach to and invade into a ZT mesothelial monolayer (green). The two cell populations were imaged every 10 minutes for 8 hours using a Nikon Ti-E Inverted Motorized Widefield Fluorescence time-lapse microscope and elements software. The graph shows that talin 1 attenuation significantly decreases mesothelial cell clearance (Quantile plot with green bars at the means).

Movie 3. Control OVCA433 spheroids (red) invading into a mesothelial monolayer (green). Click here to view movie.

Movie 4. Attenuation of talin 1 expression in OVCA433 spheroids (red) decreases mesothelial (green) clearance ability. Click here to view movie.

Discussion

The "Mesothelial Clearance Assay" presented here uses time-lapse microscopy to monitor the interactions of ovarian cancer multicellular spheroids and mesothelial cell monolayers, in great spatial and temporal detail. Previously, several groups[8-14] had used endpoint assays to show that ovarian cancer cells attach to and invade into mesothelial cell monolayers. This assay is unique in that it uses fluorescently labeled cells to distinguish tumor cells from mesothelial cells, so that the dynamics of these two cell populations can be monitored throughout the assay. The process of intercalation can be visualized in real time and the rate of mesothelial clearance can be quantitatively measured over time. The use of timelapse microscopy allows one to closely monitor the dynamics of the interaction between the two cell populations under different experimental conditions. Additionally, a small percentage of either the mesothelial cells or the ovarian cancer cells can be labeled with a third fluorescent marker to monitor the dynamics of individual cells within the population. By tracking individual cells over time, the directionality and rate of migration can be calculated. To perform higher resolution analyses of mesothelial clearance, total internal reflection fluorescence (TIRF) microscopy can be used. If focal adhesions are labeled in the mesothelial cells, the dissociation of mesothelial adhesions by protrusive extensions of the tumor cells can be monitored, as described in our previous publication[17].

This assay can be used to compare the invasion ability of ovarian cancer cell spheroids that have been genetically or pharmacologically modified to elucidate the molecular mechanisms by which ovarian cancer cell spheroids clear the mesothelial monolayer or to identify small molecule

inhibitors of the process. Furthermore, the assay requires a very small number of ovarian cancer cells, so primary tumor cells from fluid exudates can be used (see limitations below) if labeled by preincubating the cells with cytotracker dyes (Invitrogen). The assay is also amenable to high throughput analysis. To perform high throughput genetic or pharmacological studies, the ovarian cancer cells can be transfected with different siRNA vectors or treated with different pharmacological inhibitors in each well of the 96-well plate. Mesothelial cell monolayers can be plated in 96 well glass-bottom culture dishes, and the spheroids can be transferred 1:1 from the poly-HEMA coated plates to the monolayer-containing plates. All of these steps can be optimized for use with screening robots so that hundreds of siRNAs or inhibitors can screened at one time.

One of the strengths of this assay is to be able to model the force-dependent intercalation of ovarian cancer cells into the mesothelial monolayer. Our lab used traction force microscopy (TFM) to determine whether mechanical force regulates mesothelial clearance[17]. We found that overexpression of α5 integrin increased the contractility of cells plated on a fibronectin-coated substrate, while RNAi-mediated knockdown of talin, or myosin II decreased cell contractility[17]. Since downregulation of α5 integrin, talin, or myosin II in the ovarian cancer cell spheroids also decreased mesothelial clearance, our TFM measurements support the idea that mesothelial clearance in an event dependent on cellular contractile forces, in which cells with higher contractile forces caused greater mesothelial clearance. Therefore, the mesothelial clearance assay can be used to further understand intercalation events, associated with ovarian spheroid metastasis, that are dependent on mechanical forces.

This assay has a few limitations to consider. First, in order to form the multicellular spheroids, the cells must be cultured in suspension for at least 6 hours. If the cells are unable to survive without matrix contact their clearance ability will be compromised. Second, it is advantageous to use ovarian cancer cells that form uniform, compact multicellular spheroids. If the ovarian cancer cells only form loose clusters, they may break apart in the transfer from the polyHEMA-coated plate to the dish containing the mesothelial monolayer, creating spheroids of different shapes and sizes that will add variability to the data. Third, if the cells used are heterogeneous, this will add additional variability to the sizes of holes created in the monolayer. It is important to use multiple replicate wells (10-20/sample) due to the variability in extent of intercalation after eight hours. In the assays described here, well-established ovarian cancer (OVCA433) and mesothelial (ZT) cell lines were used. To make this assay more clinically relevant, primary ovarian cancer cells, from the ascites fluid of patients, can be used. It would be interesting to determine if *in vitro* mesothelial cell clearance ability correlates with clinical outcome. The limitations above are particularly important to consider when using primary samples, as the number of primary cells available is a limiting factor. Additionally, it is important to check the integrity of the mesothelial monolayer before performing this assay. The mesothelial monolayer can be fixed and stained for cell-cell junction proteins to ensure that mesothelial cell junctions are intact.

Finally, the mesothelial clearance assay can be easily modified to answer specific experimental questions. Here, we used fibronectin as the ECM component that allows the ovarian and mesothelial cells to adhere to the glass-bottom culture dishes, however, other ECM components can be used including collagen and laminin. Furthermore, other cell types that are found under the basement membrane, including fibroblasts, can be added to this experimental system, to assess the role of these cell types in mesothelial clearance[9,19,20]. Lastly, interactions of other types of tumor cells (e.g. pancreatic, breast, etc) with mesothelial cells can also be modeled using this assay. And it is feasible to study interactions between cancer cells and an endothelial monolayer, using this assay, to mimic intravasation or extravasation (Similar assays have been described in: [15,16,21-27]).

Disclosures

We have nothing to disclose.

Acknowledgements

References

1. Jemal, A., *et al.* Cancer statistics, 2009. *CA Cancer J. Clin.* **59**, 225-249, doi:caac.20006 [pii] 10.3322/caac.20006 (2009).
2. Ries, L.G, Melbert, D., Krapcho, M., Stinchcomb, D.G., Howlader, N., Horner, M.J., Mariotto, A., Miller, B.A., Feuer, E.J., Altekruse, S.F., Lewis, D.R., Clegg, L., Eisner, M.P., Reichman, M., & Edwards, B.K. In http://seer.cancer.gov/csr/1975_2005 National Cancer Institute. Bethesda, MD, (2007).
3. Burleson, K.M., *et al.* Ovarian carcinoma ascites spheroids adhere to extracellular matrix components and mesothelial cell monolayers. *Gynecol. Oncol.* **93**, 170-181, doi:10.1016/j.ygyno.2003.12.034 [pii] S0090825803009508 (2004).
4. Birbeck, M.S. & Wheatley, D.N. An Electron Microscopic Study of the Invasion of Ascites Tumor Cells into the Abdominal Wall. *Cancer Res.* **25**, 490-497 (1965).
5. Witz, C.A., Monotoya-Rodriguez, I.A., & Schenken, R.S. Whole explants of peritoneum and endometrium: a novel model of the early endometriosis lesion. *Fertil. Steril.* **71**, 56-60, [pii] S0015028298004002 (1999).
6. Zhang, X.Y., *et al.* Characteristics and growth patterns of human peritoneal mesothelial cells: comparison between advanced epithelial ovarian cancer and non-ovarian cancer sources. *J. Soc. Gynecol. Investig.* **6**, 333-340, [pii] S1071-5576(99)00040-4 (1999).
7. Kenny, H.A., Nieman, K.M., Mitra, A.K., & Lengyel, E. The First Line of Intra-abdominal Metastatic Attack: Breaching the Mesothelial Cell Layer. *Cancer Discovery.* **1**, 100-102 (2011).
8. Niedbala, M.J., Crickard, K., & Bernacki, R.J. Interactions of human ovarian tumor cells with human mesothelial cells grown on extracellular matrix. An *in vitro* model system for studying tumor cell adhesion and invasion. *Exp. Cell. Res.* **160**, 499-513 (1985).

9. Kenny, H.A., Krausz, T., Yamada, S.D., & Lengyel, E. Use of a novel 3D culture model to elucidate the role of mesothelial cells, fibroblasts and extra-cellular matrices on adhesion and invasion of ovarian cancer cells to the omentum. *Int. J. Cancer.* **121**, 1463-1472, doi:10.1002/ijc.22874 (2007).
10. Ksiazek, K., *et al.* Senescent peritoneal mesothelial cells promote ovarian cancer cell adhesion: the role of oxidative stress-induced fibronectin. *Am. J. Pathol.* **174**, 1230-1240, doi: 10.2353/ajpath.2009.080613 [pii] S0002-9440(10)60982-0 (2009).
11. Burleson, K.M., Boente, M.P., Pambuccian, S.E., & Skubitz, A.P. Disaggregation and invasion of ovarian carcinoma ascites spheroids. *J. Transl. Med.* **4**, 6, doi: 10.1186/1479-5876-4-6 [pii] 1479-5876-4-6 (2006).
12. Heyman, L., *et al.* Vitronectin and its receptors partly mediate adhesion of ovarian cancer cells to peritoneal mesothelium *in vitro*. *Tumour. Biol.* **29**, 231-244, doi: 10.1159/000152941 [pii] 000152941 (2008).
13. Heyman, L., *et al.* Mesothelial vitronectin stimulates migration of ovarian cancer cells. *Cell. Biol. Int.* **34**, 493-502, doi:10.1042/CBI20090331 [pii] CBI20090331(2010).
14. Lessan, K., Aguiar, D.J., Oegema, T., Siebenson, L., & Skubitz, A.P. CD44 and beta1 integrin mediate ovarian carcinoma cell adhesion to peritoneal mesothelial cells. *Am. J. Pathol.* **154**, 1525-1537, [pii] S0002-9440(10)65406-5 (1999).
15. Leroy-Dudal, J., Heyman, L., Gauduchon, P., & Carreiras, F. Adhesion of human ovarian adenocarcinoma IGROV1 cells to endothelial cells is partly mediated by the alphav integrins-vitronectin adhesive system and induces an alteration of endothelial integrity. *Cell. Biol. Int.* **29**, 482-488, doi: 10.1016/j.cellbi.2005.01.008 [pii] S1065-6995(05)00048-X (2005).
16. Leroy-Dudal, J., *et al.* Transmigration of human ovarian adenocarcinoma cells through endothelial extracellular matrix involves alphav integrins and the participation of MMP2. *Int. J. Cancer.* **114**, 531-543, doi:10.1002/ijc.20778 (2005).
17. Iwanicki, M., *et al.* Ovarian cancer spheroids use myosin-generated force to clear the mesothelium. *Cancer Discovery.* **1**, 144-157 (2011).
18. Folkman, J. & Moscona, A. Role of cell shape in growth control. *Nature.* **273**, 345-349 (1978).
19. Gregoire, L., Munkarah, A., Rabah, R., Morris, R.T., & Lancaster, W.D. Organotypic culture of human ovarian surface epithelial cells: a potential model for ovarian carcinogenesis. *In Vitro Cell Dev. Biol. Anim.* **34**, 636-639 (1998).
20. Roberts, P.C., *et al.* Sequential molecular and cellular events during neoplastic progression: a mouse syngeneic ovarian cancer model. *Neoplasia.* **7**, 944-956 (2005).
21. Okada, T., Okuno, H., & Mitsui, Y. A novel *in vitro* assay system for transendothelial tumor cell invasion: significance of E-selectin and alpha 3 integrin in the transendothelial invasion by HT1080 fibrosarcoma cells. *Clin. Exp. Metastasis.* **12**, 305-314 (1994).
22. Zervantonakis, I.K., Kothapalli, C.R., Chung, S., Sudo, R., & Kamm, R.D. Microfluidic devices for studying heterotypic cell-cell interactions and tissue specimen cultures under controlled microenvironments. *Biomicrofluidics.* **5**, 13406, doi:10.1063/1.3553237 (2011).
23. Brandt, B., *et al.* 3D-extravasation model -- selection of highly motile and metastatic cancer cells. *Semin. Cancer Biol.* **15**, 387-395, doi: 10.1016/j.semcancer.2005.06.006 [pii] S1044-579X(05)00039-8 (2005).
24. Condeelis, J. & Segall, J.E. Intravital imaging of cell movement in tumours. *Nat. Rev. Cancer.* **3**, 921-930, doi:10.1038/nrc1231 [pii] ncr1231 (2003).
25. Dai, J., Ting-Beall, H.P., Hochmuth, R.M., Sheetz, M.P., & Titus, M.A. Myosin I contributes to the generation of resting cortical tension. *Biophys. J.* **77**, 1168-1176 (1999).
26. Laferriere, J., Houle, F., Taher, M.M., Valerie, K., & Huot, J. Transendothelial migration of colon carcinoma cells requires expression of E-selectin by endothelial cells and activation of stress-activated protein kinase-2 (SAPK2/p38) in the tumor cells. *J. Biol. Chem.* **276**, 33762-33772, doi:10.1074/jbc.M008564200 [pii] M008564200 (2001).
27. Dong, C., Slattery, M.J., Rank, B.M., & You, J. *In vitro* characterization and micromechanics of tumor cell chemotactic protrusion, locomotion, and extravasation. *Ann. Biomed. Eng.* **30**, 344-355 (2002).